Article

Applying the SIMPLE Crop Model to Assess Soybean (*Glicine max.* (L.) Merr.) Biomass and Yield in Tropical Climate Variation

Quang V. Pham [1,2], Tanh T. N. Nguyen [2,3,4,*], Tuyen T. X. Vo [1,2], Phuoc H. Le [1,2], Xuan T. T. Nguyen [1,2], Nha V. Duong [5] and Ca T. S. Le [2,3]

[1] Faculty of Agriculture and Natural Resources, An Giang University, 18 Ung Van Khiem St., Long Xuyen City 90000, An Giang Province, Vietnam; pvquang@agu.edu.vn (Q.V.P.)
[2] Vietnam National University Ho Chi Minh City, Linh Trung Ward, Thu Duc District, Ho Chi Minh City 71300, Vietnam
[3] Faculty of Engineering, Technology and Environment, An Giang University, 18 Ung Van Khiem St., Long Xuyen City 90000, An Giang Province, Vietnam
[4] Climate Change Institute, An Giang University, 18 Ung Van Khiem St., Long Xuyen City 90000, An Giang Province, Vietnam
[5] Faculty of Agriculture and Rural Development, Kien Giang University, 320A, 61 National Highway, Minh Luong Town, Chau Thanh District 91700, Kien Giang Province, Vietnam
* Correspondence: ntntanh@agu.edu.vn

Abstract: Soybean *Glicine max.* (L.) Merr. is one of the most major food crops. In some areas, its responses to different climates have not been well studied, particularly in tropical countries where other crops are more dominant. Accordingly, we adopted the SIMPLE crop model to investigate the responses of soybeans to the climate. We conducted two experiments on crop growth in the Summer–Autumn season of 2020, and Winter–Spring 2021 in the Hoa Binh Commune, in the Mekong Delta, Vietnam, which is an area that is vulnerable to climate change impacts, to obtain data for our model input and assessment. The assessment was concerned with the effects of climate variables (temperature and CO_2) on soybean biomass and yield. The results indicated that the SIMPLE model performed well in simulating soybean yields, with an RRMSE of 9–10% overall. The drought stress results showed a negative impact on the growth and development of soybeans, although drought stress due to less rainfall seemed more serious in Spring–Winter 2021 than in Summer–Autumn 2020. This study figured out the trend that higher temperatures can shorten biomass development and lead to yield reduction. In addition, soybeans grown under high CO_2 concentrations of 600 ppm gave a higher biomass and a greater yield than in the case with 350 ppm. In conclusion, climate variance can affect the soybean yield, which can be well investigated using the SIMPLE model.

Keywords: SIMPLE; soybean biomass and yield; climate change; modeling

1. Introduction

Climate varies over time and can cause problems for food crops. For this reason, an assessment of the responses of crops to the climate is needed, particularly for major food crops. Soybean, a leguminous annual C3 plant in the Fabaceae family [1], is a food crop that has caused much concern due to its nutritional values for animals and humans. Soybean responses to the climate have been widely studied, but the investigation of the responses in tropical areas is uncommon. For countries where soybean is not a major crop, knowledge of soybean responses is rarely known.

Previous studies have reported the key effects of climatic factors on soybeans. For instance, the temperature can affect the soybean yield [2]; for example, an increase of 1 °C in summer led to a decrease in the yield by 16% in Wisconsin, USA [3]. For Rio Grande do Sul (southern Brazil), a subtropical area, water supply and photothermal quotient are the factors that cause yield variation [4]. As reported in the study in Matopiba, Brazil, the

sowing date (in relation to climate) is the determinant of the yield changes [5]. Yield can also be affected by photoperiod and crop management, which were found in sub-Saharan Africa [6].

The soybean yield can be assessed using crop models. The models may require a large number of parameters [7], and they have particular designs and set-up, which can constrain the model and the assessment of the effects of climate change on crops. Due to model design, study purposes, and input data requirements, the applicability of the models is varied, particularly for soybeans. For instance, the model DSSAT/CROPGRO-Soybean was useful for estimating the soybean yield (i.e., in Matopiba, Brazil [5]) and the optimal management (i.e., in Phu Pha Man, Thailand [8]). ORCHIDEE-CROP, a process-oriented terrestrial biogeochemical model based on generic crop phenology [9] performs well for soybean yield simulation in China [10]. EPIC-Boku helps envision the negative effect of temperature on the yield [11]. In addition, EPIC-IIASA is applicable for studying the effects of CO_2 on yields in Argentina, Brazil, and the USA [12]. Process-based models can be coupled with artificial intelligence for crop assessment, i.e., machine learning links GEPIC to assess the effects of climate change on soybean in Argentina, Brazil, China, and the USA [13], and the application of artificial neural networks for the yield estimation in Maryland, USA [14]. The models are different from each other but geographically dependent, and thus their simulation performance levels are various. In addition, models may require many data inputs that are somehow not available; therefore, simplified models with satisfactory performance are preferred for soybean studies.

Tropical areas have particular climatic characteristics that influence soybean growth. Hence, an assessment of its responses to climate is needed to determine which crop models can help. Among tropical countries, Vietnam is currently under climatic threat [15], which is an ideal study case for the assessment. In this region, the Mekong River Delta (MRD) is widely known for being severely affected by extreme droughts [16]. Studying the responses in this area may help fulfill the knowledge of the responses to climate for decision-making. The current investigations of this crop in this area are more experimental but less modeling. Although the crop models above may be applicable to the assessment, their applications are limited. In addition, since soybean is not a major crop, studies on its responses to climate are rare, and so the input data for modeling is not always available; this issue constrains the application of these models.

In regards to data availability and climate in the Mekong Delta, Vietnam, this study adopted the SIMPLE model with simplified and open-sourced designs that performed well in terms of soybean yield estimation for temperate areas in the USA [7]. Through this pilot study, we assessed the yield and biomass of the soybean (*Glycine max.* (L.) Merr.) and then informed the model's applicability and the effects of climate variation on the crop, which is necessary to help protect this crop in the context of climate change. Therefore, this study aims at (1) adopting the SIMPLE model for soybean biomass and yield estimation, and (2) using the model to assess the soybean biomass and yield under climate change in temperature and CO_2. Our final goal is to investigate how climate variation affects soybean yield to contribute to crop and food protection.

2. Methods

2.1. Field Experiments

The purpose of field experiments was to obtain data for model input supply (including parameters), model calibration, and assessment. This study includes two field experiments on soybean cultivation in 2020 and 2021. The study field is based in Hoa Binh Commune, Cho Moi district, An Giang province, Vietnam (10°23′47″ N, 105°27′41″ E), with existing soybean cultivation (Figure 1) and clay loam soil with an organic matter content of 1.6% (Table 1). In our experiments, the soybean was grown in rainy season (July to October 2020) and dry season (January to April 2021). Three soybean seeds were sown in a hole, row by row at 35 cm and plant to plant at 25 cm. After emergence, plants were thinned to one per hole. To focus on climate effects, this study used the common fertilizing including

55 kg N, 75 kg P_2O_5, and 40 kg K_2O per hectare and pesticide application schedule currently practiced in the region. The field measurement includes the following data:

- Sowing date, flowering date, maturity date, and growing time.
- Plant height (cm), leaves number, total vegetative biomass (t ha^{-1}) per 10 days. vegetative biomass (t ha^{-1}), and grain yield.
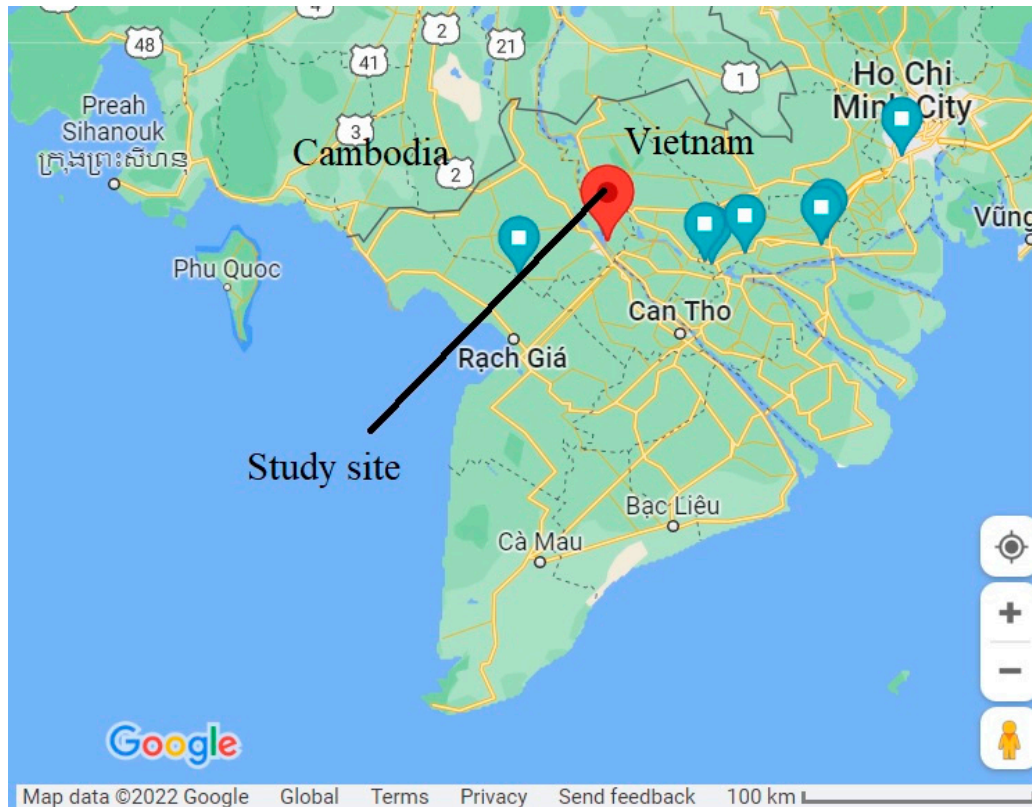

Figure 1. Study location.

Table 1. Summary of the climatic features in the experiment site.

Climatic Features	Year	
	2020	**2021**
Total rainfall (mm)	874.1	89.1
Number of rainy days	62.0	38.0
Mean temperature (°C) *	30.5	29.0
Mean radiation (MJ m^{-2}d^{-1}) **	15.8	19.7

*: recorded by Thermo Recorder TR-72Ui (T&D Corp, Japan). **: data from the Agroclimatology Community of the POWER Data Access Viewer.

The soybean cultivar used in the experiment was a high-yielding variety (DT2006). Soil properties in field for the experiments are shown in Table 2.

Table 2. Soil properties at the research site.

Items	Characteristics
Soil texture	
Sand (%)	30
Silt (%)	42
Clay (%)	28

Table 2. *Cont.*

Items	Characteristics
Soil properties or soil parameters	
Total nitrogen (%)	0.17
Total phosphorus (%P_2O_5)	0.03
Exchangeable potassium (cmol kg^{-1})	0.23
Field capacity (cm^3 cm^{-3})	0.18
Available water capacity—AWC (cm^3 cm^{-3})	0.14
Runoff curve number—RCN	84
Deep drainage coefficient—DDC	0.18
Root zone—RZD (mm)	329
Ground water level (cm)	35.8
Fertilizer applied	
N (kg)	55
P (kg)	75
K (kg)	80

2.2. Modeling of Soybean Yield

This study used the SIMPLE model [7] (with daily timestep) based on crop physiology with a few parameters and equations. We assume that nutrients are given enough for soybean, and thus, this does not account for the effects of fertilizers on its growth. In this sense, this model is appropriate for assessing the climatic effects. This model considers crop yield as the product of the harvest index (HI) and the fraction of the above-ground cumulative biomass from sowing to maturity:

$$Yield = Biomass\_cum \times HI \tag{1}$$

where *HI* is the harvest index, the ratio of grain to total dry matter, and *Biomass_cum* is calculated using the following Euler approach:

$$Biomass\_cum_{i+1} = Biomass\_cum_i + Biomass\_rate_i \tag{2}$$

Biomass_rate$_i$ is the daily biomass growth rate, and *Biomass_cum$_i$* is the cumulative biomass. *Biomass_rate$_i$* is determined in Equation (3), which depends on radiation use efficiency (RUE) of the plant canopy that intercepts daily photosynthesis active radiation (PAR) [17]. The daily change in plant biomass is affected by stress variables such as high temperatures, drought, and atmospheric CO_2 concentration [18].

$$Biomass_{rate} = \begin{matrix} Radiation \times f(Solar) \times RUE \times f(CO_2) \times f(Temp) \\ \times \min((f(Heat), f(Water)) \end{matrix} \tag{3}$$

where $f(Solar)$ is the fraction of the solar radiation intercepted by the crop canopy regarding the Beer–Lambert law of light attenuation [19] (as cited in Zhao et al., 2019), $f(CO_2)$ is the CO_2 impact, $f(Heat)$ is the heat stress function, and $f(Water)$ is the water stress function [7,18].

$f(Solar)$ for leaf growth and senescence period is as follows:

$$f(Solar) = \begin{cases} \frac{f_{Solar\_max}}{1+e^{-0.01(TT-I_{50A})}}, leaf\ growth\ period \\ \frac{f_{Solar\_max}}{1+e^{-0.01(TT-(T_{sum}-I_{50B}))}}, leaf\ senescence\ period \end{cases} \tag{4}$$

where I_{50A} is the cumulative temperature needed for leaf area development to intercept 50% of solar radiation during canopy closure; I_{50B} is the cumulative temperature needed from maturity to 50% of radiation interception during canopy senescence. f_{Solar_max} is the maximum fraction of radiation interception. f_{Solar_max} is used to account for different plant

spacings. For most high-density crops, this value is set at 0.95 [7]. *TT* is the cumulative mean temperature, which is calculated as follows:

$$\Delta TT = \begin{cases} T - T_{base}, & T > T_{base} \\ 0, & T \leq T_{base} \end{cases} \tag{5}$$

$$TT_{i+1} = TT_i + \Delta TT \tag{6}$$

where TT_i is the cumulative mean temperature of *i*th day, ΔTT is the daily added mean temperature, *T* is the daily average temperature (TMAX + TMIN)/2, and T_{base} is the base temperature for crop growth and phenological development [7,18].

Temperature stress, heat stress, drought stress, water stress, and CO_2 impact are calculated regarding the suggestions of [7,20–26].

$$f(Temp) = \begin{cases} 0, & T < T_{base} \\ \frac{T - T_{base}}{T_{opt} - T_{base}}, & T_{base} \leq T < T_{opt} \\ 1, & T \geq T_{opt} \end{cases} \tag{7}$$

where *T* is the daily mean temperature, and T_{base} and T_{opt} are the base and optimal temperature for biomass growth, respectively, for a given crop species.

$$f(Heat) = \begin{cases} 1, & T_{max} \leq T_{heat} \\ 1 - \frac{T - T_{base}}{T_{opt} - T_{base}}, & T_{heat} < T_{max} \leq T_{extreme} \\ 0, & T_{max} > T_{extreme} \end{cases} \tag{8}$$

where T_{max} is the daily maximum temperature, T_{heat} is the threshold temperature when biomass growth rate starts to be reduced by heat stress, and $T_{extreme}$ is the extreme temperature threshold when the biomass growth rate reaches 0 due to heat stress.

$$f(CO_2) = \begin{cases} 1 + S_{CO_2}(CO_2 - 350), & 350\,\text{ppm} \leq CO_2 < 700\text{ppm} \\ 1 + 350.S_{CO_2}, & CO_2 > 700\text{ppm} \end{cases} \tag{9}$$

where S_{CO_2} is the crop-specific sensitivity of RUE to elevated CO_2, and CO_2 is the atmospheric CO_2 concentration.

$$f(water) = 1 - S_{water} \times ARID \tag{10}$$

ARID is a standardized index ranging from 0 (no water shortage) to 1 (extreme water shortage and associated drought stress). *ARID* is calculated based on water availability and reference evapotranspiration (Eto). S_{water} is the sensitivity of RUE to the ARID index.

$$ARID = 1 - \frac{\min(ETo, 0.096PAW)}{ETo} \tag{11}$$

PAW is plant-available water content in the soil profile for the rooting depth and is obtained from a simple water balance function, including precipitation, irrigation, surface runoff, and deep drainage (see [26] for more details). *ETo* is the reference evapotranspiration, which is calculated using the Priestley and Taylor approach [23]. The drought stress function is similarly described by Sinclair et al. [27]. Crop stress occurs when the proportion of plant available water is smaller than 75%.

The radiation interception depends on drought stress:

$$I_{50B,\ i+1} = I_{50B,\ i} + I_{max,\ water} \times (1 - f(Water)) \tag{12}$$

where $I_{max,\ water}$ is the maximum daily increase in I_{50B} due to drought stress.

The radiation interception is affected when the drought stress becomes severe enough [28].

$$fSolar\_water = \begin{cases} 0.9 + f(Water), \ f(Water) \leq 0.1 \\ 1, \ f(Water) > 0.1 \end{cases} \tag{13}$$

2.3. Model Parameters and Inputs

This study used thirteen parameters to run the SIMPLE model (Table 3), including cultivar characteristics. T_{sum}, I_{50A}, and I_{50B} were determined from the observations of experiment data and the air temperature data. The HI was calculated as described in [29]. The remaining parameters were obtained from the literature.

Table 3. Model parameters.

Name	Description	Range	Note
Cultivars parameters			
T_{sum}	Thermal time requirement from sowing to maturity in daily mean (°C days).	2070–2300	*
HI	Harvest index.	0.30–0.37	*
I_{50A}	Thermal time requirement after sowing fraction of light interception to reach 50% (°C days).	500–710	*
I_{50B}	Represents natural senescence. Thermal time requirement from maturity backwards for light interception to reach 50% (°C days).	200–250	*
Species parameters			
T_{base}	Base temperature (daily mean T) for phenology development and growth (°C).	6–10	[30]
T_{opt}	Optimal temperature (daily mean T) for biomass growth (°C).	25–30	[31]
RUE	Radiation use efficiency (above ground biomass and below ground, if harvestable, product is below ground) (g MJ^{-1}m^{-2}).	0.85–1.60	[32]
I_{50maxH}	The maximum daily increase in I50B due to heat stress (°C d).	120	[7]
I_{50maxW}	The maximum daily increase in I50B due to water stress (°C d).	20	[7]
MaxT	Threshold for daily Tmax to start accelerating senescence due to heat stress (°C).	40	[33]
ExtremeT	Daily Tmax threshold when RUE becomes 0 due to heat stress (°C).	25–40	[33]
CO_2_RUE	Relative increase in RUE per 1 ppm elevated CO_2 above 350 ppm.	350–600	[7]
S_Water	Sensitivity of RUE to drought stress (ARID index).	0.6–0.96	[7]

Notes: * data obtained from experiments in this study.

Data calibration and validation of the model were implemented by carrying out a number of simulations using cultivar parameter sets within a reasonable range (excluding soil parameter, which was kept the same for all the trials). In both two experiments, the biomass was measured periodically every 10 days from sowing to maturity date. The observed data were used to validate the simulation outputs. T_{sum} (cumulative daily mean temperature above T_{base}) was set so that canopy cover at harvest date was about 80% [7]. After each model run, I_{50A} and I_{50B} were recalibrated based on daily mean temperature above T_{base} and iterative simulations until a good fit to the experimental results was achieved. Then, the best-fit set of cultivar parameters was used for scenario analysis.

Input variables required to run the SIMPLE model include weather (daily maximum/minimum temperature, rainfall, and solar radiation), atmospheric CO_2 concentration, sowing/harvesting date, irrigation, initial variables, and four variables characterizing

the soil (Tables 2 and 3), including fraction of plant's available water-holding capacity (AWC; one number for entire soil profile, limited by rooting depth), runoff curve number (RCN), deep drainage coefficient (DDC), and root zone depth (RZD, a fixed maximum depth) (Table 4).

Table 4. Input variables of SIMPLE model adapted from Zhao et al. [7].

Input Variables	Description	Unit
Crop management	Sowing date (SowingDate)	-
	Harvesting date (HarvestDate)	-
	Irrigation depth (Irri)	m
Initial	Biomass (InitialBio)	Ton
	Cumulative temperature (InitialTT)	°C day
	Solar radiation interception (InitialFsolar)	-
Soil characteristics	Atmospheric CO_2 concentration	ppm
	Soil water-holding capacity (AWC)	-
	Runoff curve number (RCN)	-
	Deep drainage coefficient (DDC)	-
	Root zone depth (RZD)	m
Weather	Daily maximum temperature (TMAX)	°C
	Daily minimum temperature (TMIN)	°C
	Daily rainfall amount (RAIN)	m
	Daily solar radiation (SRAD)	MJ m^{-2} day^{-1}

The daily solar radiation (MJ m^{-2} day^{-1}) was collected from the Agroclimatology Community of the POWER Data Access Viewer for a period of 2 years from 2020 to 2021 at the experiment location (Figure 1). Air temperature was recorded by Thermo Recorder TR-72Ui (T&D Corp, Japan) and adapted from the POWER Data Access Viewer by the NASA Langley Research Center (LaRC) POWER Project funded through the NASA Earth Science/Applied Science Program (https://power.larc.nasa.gov/data-access-viewer/ (accessed on 1 August 2022)).

2.4. Model Assessment

Calibration was performed using the measured datasets and validation of the model was performed using measured datasets of the cropping seasons of the year 2020 and 2021. The model assessment was conducted using the root mean square of error (RMSE) criterion (Equation (14)).

$$RMSE = \sqrt{\frac{\sum_{i=1}^{n}(Y_{sim,i} - Y_i)^2}{n}} \qquad (14)$$

where $Y_{sim,i}$ is simulated yield, Y_i is observed yield, i is the data index, and n is the length of data. After that, this study calculated *RRMSE*, which is relative *RMSE* by dividing *RMSE* with average value of measured data as follows:

$$RRMSE = \frac{RMSE}{\sum_{i=1}^{n} Y_i} \times 100\% \qquad (15)$$

where *RRMSE* < 10%, 10% < *RRMSE* < 20%, 20% < *RRMSE* < 30%, and *RRMSE* > 30% indicate excellent, good, fair, and poor models, respectively [34].

2.5. Scenario Analysis

The set of parameters that gave the best fit between simulation and observation was used as a control treatment to generate scenarios for the purpose of better understanding the impact of future climate change on agricultural production. Scenario analysis was implemented with the following incremental changes in mean temperature change: +1 °C,

+2 °C, +3 °C, +4 °C, and +5 °C and the following atmospheric CO_2 concentration changes: +50 ppm, +100 ppm, +150 ppm, +200 ppm, and +250 ppm.

3. Results and Discussions

3.1. Model Assessment

The model evaluation results showed that the SIMPLE model was applicable to estimate the biomass and grain yield of soybean. The simulated biomass fit well to the observed biomass for the two crops (Figure 2). The simulated growing season length was 96 days for Summer–Autumn 2020 and 88 days for Spring–Winter 2021; this is consistent with that of the soybean cultivar used for the experiments (85–95 days). Significantly positive relationships were found between the observed and simulated yields for the Summer–Autumn 2020 season (Figure 3a) and the Spring–Winter 2021 season (Figure 3b).
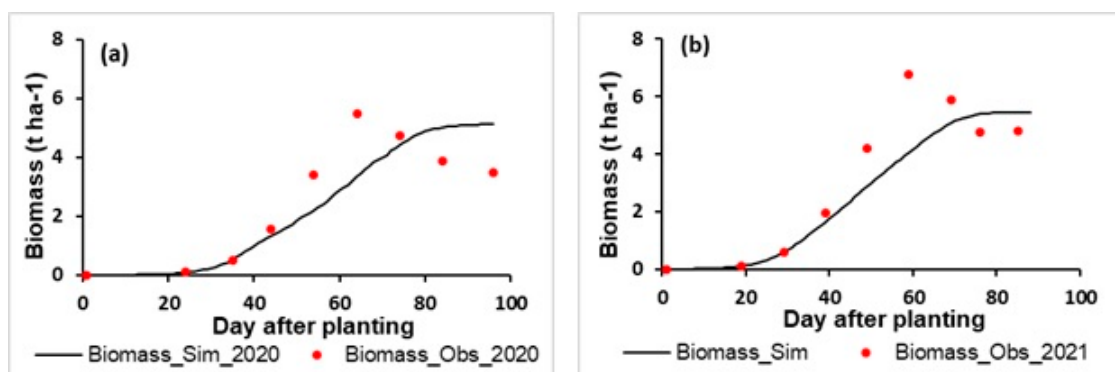

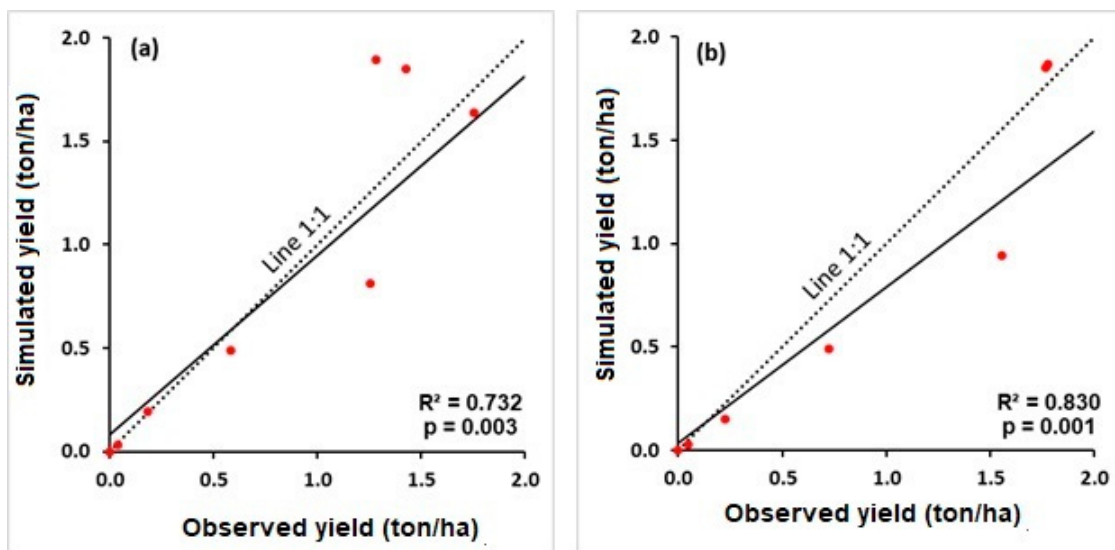**Figure 2.** Total simulated and observed biomass for Summer–Autumn season 2020 (**a**) and Spring–Winter season 2021 (**b**).

Figure 3. Simulated vs. observed yield for the Summer–Autumn season 2020 (**a**) and the Spring–Winter season 2021 (**b**).

The results show that the biomass and yield were well simulated using the SIMPLE model (Table 5). In this study, model performance testing resulted in an RRMSE of 9–10% overall for the biomass and yield, which indicates that the applied SIMPLE model is an excellent model regarding the category described by Jamieson et al. [34]. In a similar case study in the USA for soybeans with the same modeling approach, the obtained RRMSE value was about 25.4% [7], which is higher than in our case. Models simulating soybean

yields may perform in various ways (regarding RRMSE values), which depends on the data availability and study location. For instance, the RRMSE was 3% for the model AquaCrop for the case in Ile-Ife, Nigeria [35] while 20% for the model CROPGRO-Soybean in northeast China [36]. The performance may also rely on modeling approaches. For instance, SAFY with satellite data of leaf area index (LAI) can help obtain the soybean yield in the southwest of France with an RRMSE of 2.5%, while coupling Sentinel-2 LAI with crop modeling can result in an RRMSE of 35.8% overall for the case in Uruguay [37]. Results from this study show that the adapted SIMPLE model is proper for soybean biomass and yield estimation.

Table 5. Observed and simulated biomass and yields.

Season Crop	Observation (t ha^{-1})		Simulation (t ha^{-1})	
	Biomass	**Yield**	**Biomass**	**Yield**
2020	4.801	2.101	5.005	1.852
2021	4.739	2.225	5.466	2.023

3.2. Effects of Climate Variation

3.2.1. Growth Stages

This study figured out the growing season and growth stages of soybean observed from the two experiments in 2020 and 2021 (Table 6). The results showed that the growth stages for the Summer–Autumn season 2020 were almost longer compared to the Spring–Winter 2021, with a variation from 1 to 7 days, depending on each stage of growth.

Table 6. Growth stages of soybean crop in 2020 and 2021.

Stages	Year	
	2020	**2021**
Growing period	21 July to 24 October	20 January to 17 April
Bloom	20 August (31 DAP)	18 February (30 DAP)
Seed fill	2 September (44 DAP)	28 February (40 DAP)
Mat	12 October (84 DAP)	7 April (78 DAP)
Harvest date	25 October (96 DAP)	17 April (88 DAP)

Note: DAP—day after planting.

3.2.2. Rainfall and Drought

The weather pattern at the experimental site, in general, was different between the Summer–Autumn season in 2020 and the Spring–Winter season in 2021, especially concerning the rainfall amount and the number of rainy days, which are also similar to solar radiation (Table 1 and Figure 4). This may affect the biomass and yield of the soybean crop. The total biomass of the Summer–Autumn 2020 growing season was 4.801 t ha^{-1}, which was slightly higher than that in the Spring–Winter 2021 (4.739 t ha^{-1}) (Table 5). The yield was 2.101 t ha^{-1} and 2.225 t ha^{-1} for the Summer–Autumn 2020 and the Spring–Winter 2021, respectively (Table 5).

More rainfall concentrated during 10–21 and 56–90 days after planting for the 2020 period (Table 1 and Figure 4b), which may prolong the vegetative and R5–R7 stages, and thus lead to the delay of blooming and development, which was similar to [38]. Aberrant rainfall may shorten or extend the flowering stage [39]. In addition, the solar radiance was lower than that in the Spring–Winter 2021 (Figure 4a) and thus this may result in the reduction of solar radiation use efficiency (RUE) and finally the yield.

Drought stress can affect crop growth. The findings in this study reported that the drought stress simulated by the SIMPLE model was low to medium during the whole season for both experiments, especially during the 6–84 days after planting for the Spring–Winter season 2021 (Figure 5a,b). The drought stress was higher during the first 10 days and 27–54 days after planting in the Summer–Autumn 2020, f(Water) ranged from 0.44 to

1.0, while for the Spring–Winter season of 2021, f(Water) ranged from 0.52 to 1.0 and widely distributed during almost all growth stages of the plant. Overall, drought stress had a relative effect on the growth and development of the soybean; however, during the Spring–Winter 2021 it seems to be more serious than the Summer–Autumn 2020 because it is usually less rainy in the dry season (from November to the end of April in the Mekong delta).
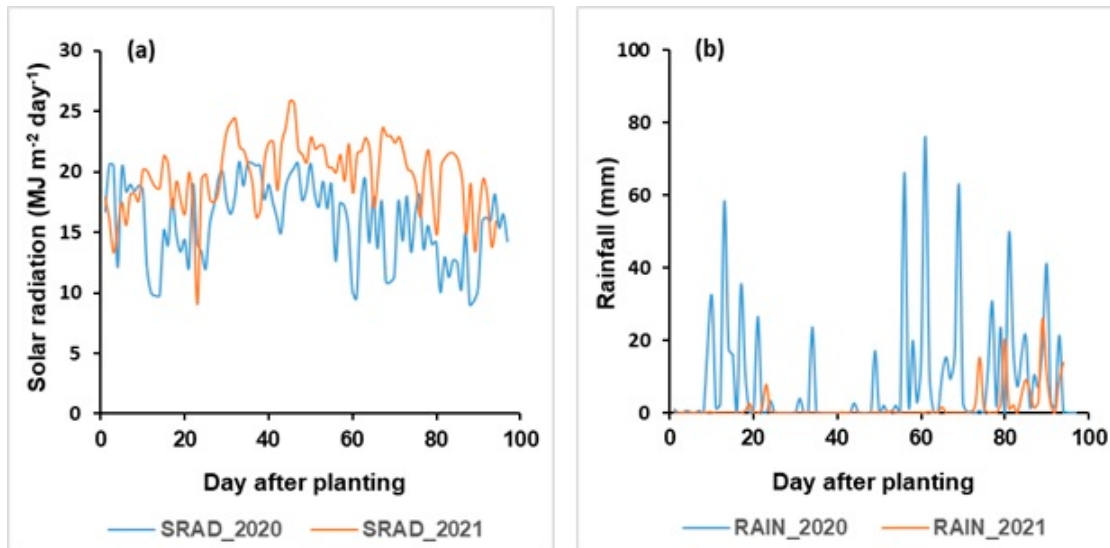

Figure 4. Daily solar radiation (**a**) and rainfall (**b**) for Summer–Autumn season 2020 and Spring–Winter season 2021.
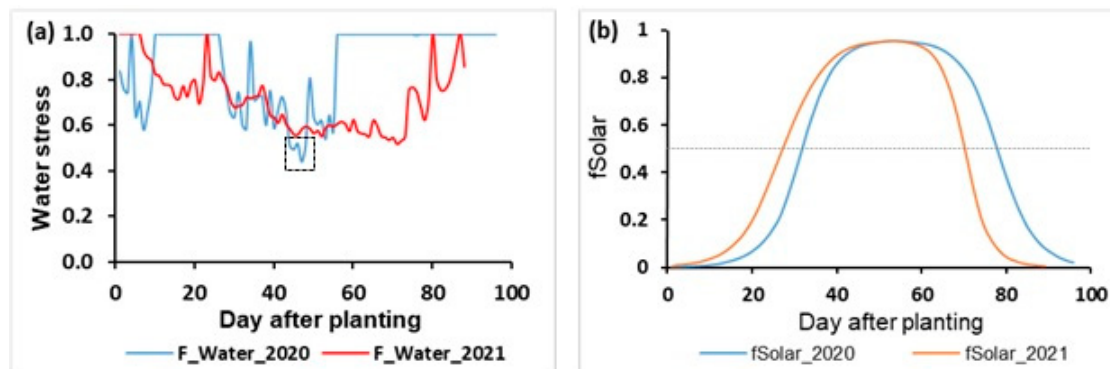

Figure 5. Water stress index (**a**) and simulated fraction of intercepted photosynthesis active radiation—fSolar (**b**) for Summer–Autumn 2020 and Spring–Winter 2021.

More rainfall during the late stage may cause the green canopy to be maintained for a longer period of time and result in a decrease in time from maturity backwards for the light interception to reach 50%; this means that the value of I_{50B} becomes lower, and therefore, the initial development and middle stages may need more time to be completed. It was quite clearly reflected in the dynamics of the fraction of radiation interception (fSolar) in the SIMPLE model (Figure 6b). As shown in Figure 6b, increasing I_{50B} caused an acceleration of canopy senescence and consequently led to the maturity date for the Spring–Winter 2021 being advanced by about 7 days compared to the Summer–Autumn 2020. The impact of heat stress is similar to that of drought stress.
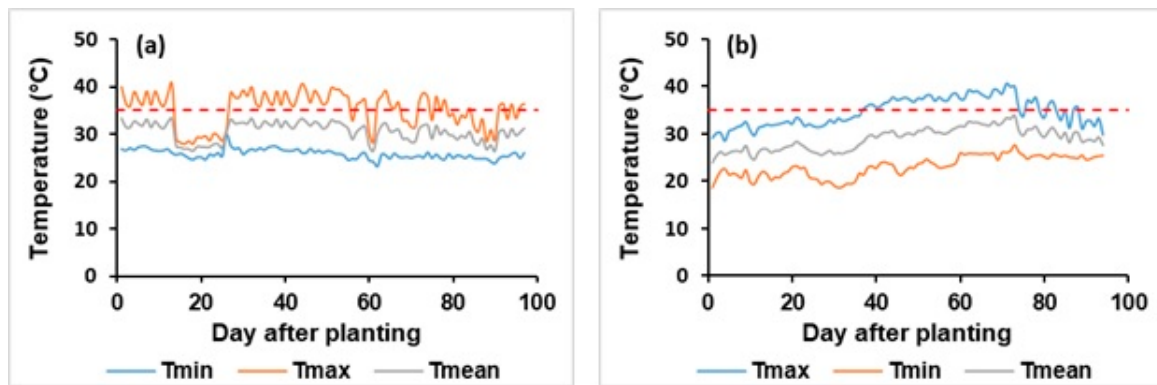
Figure 6. Daily temperature for Summer–Autumn season 2020 (**a**) and Spring–Winter season 2021 (**b**).

3.2.3. Temperature Effects

The observed daily temperature varied from 29.8 °C to 40.7 °C for Summer–Autumn season 2020 (Figure 6a), and from 23.2 °C to 34.7 °C for the Spring–Winter 2021 (Figure 6b). The average daily temperature in the Summer–Autumn 2020 crop (30.5 °C) was slightly higher than that in the Spring–Winter 2021 (29.0 °C). Particularly, the number of days in which maximum temperature above 35 °C were 62 days (Figure 6a) and 44 days (Figure 6b) during the growing seasons; thus, the extended time of maximum temperature was also longer and quite higher than that in the Spring–Winter 2021.

The total simulated biomass dynamics for the two crop seasons are shown in Figure 7. The results from the SIMPLE model showed that a temperature increase caused a significant decline in the final cumulative biomass. The yield declined by approximately 32% and 14% compared with the observed yield for the Summer–Autumn and the Spring–Winter 2021 periods, respectively.
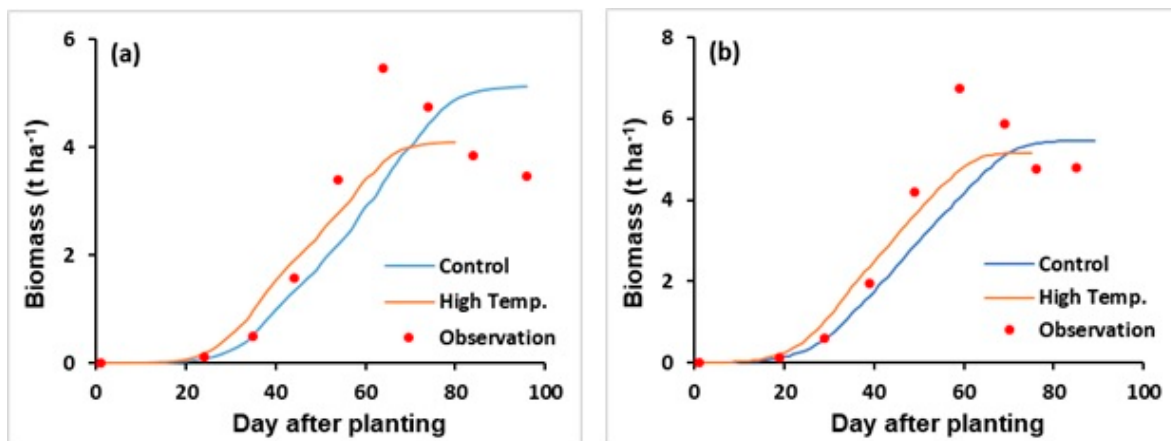

Figure 7. Total aboveground biomass under different atmospheric temperature for the control and high temperature, and observed total biomass from the experiment site. (**a**) Summer-Autumn 2020; (**b**) Spring-Winter 2021.

The findings from this study show that temperature significantly affects the soybean yield, and an elevated temperature can cause a yield reduction. As reported, mid- and high-latitude areas may benefit from warming temperatures, in which the warming outside of the core of the growing season is the most beneficial to the yield increase [3]. However, the benefit of warming depends on how soybeans respond to the change. Indeed, this study shows that the increase in temperature can lead to a yield reduction, which was similarly reported in the case in the USA [7]. The effect of temperature on soybeans is caused by their physiological characteristics. The optimum growth takes place at temperatures between 20

and 30 °C [40]. The yield gradually increases with temperatures up to 29 °C to 32 °C and then sharply decreases as temperatures exceed this threshold [41]. In another case, seed set on sterile male and fertile female soybeans decreased as the daytime temperatures increased from 30 to 35 °C [42], which was alsoS mentioned by Caviness and Fagala [43]. Overall, a sustained increase in ambient temperature would likely threaten soybean yields [44].

This study confirms the effects of temperature on the yield. The analyses of 51 stations in China from 1992 to 2011 showed that an increasing temperature can change soybean phenology and shorten its growth stages [45]. For this reason, warming temperatures may reduce the yield of soybeans [46]. For instance, a canopy temperature over 20.9 °C in central Illinois can lead to a yield reduction [47]. As predicted, climate change (primarily temperature change) may result in potential yield losses in the USA, Russia, and India by 15.1–16.1% by the end of the 21st century [48]. This spectrum could also be a potential problem in Matopiba, Brazil, where meets the predicted yield reductions of over 23% under RCP 8.5 (2041–2070) due to temperature increases above 3 °C [49]. In principle, the warming temperature during pod filling can inhibit transgenerational seed germination, particularly for 37 °C/29 °C (day/time) [50] and then cause a reduction in the seed mass, seeds per pod, and seeds per plant [47]. For soybean genotype EC 538828, high temperatures up to 42/28 °C (day/night) can decrease its photosynthesis, stomatal conductance, and seed yield [51]. The evidence above implies that tropical areas, such as Vietnam, with potential temperature increases in the future can encounter risks of the yield reduction. For this reason, climate change adaptations in this area should consider not only soybean genotypes that are tolerant to high temperatures [50] but also cultivation areas (with climatic conditions) [48]. Since the yield is dependent on temperature, future adaptations to this issue should consider selecting proper planting dates to avoid temperature extremes [52]; in other words, a cropping calendar change.

3.2.4. CO_2 Fertilization Effect

This study simulated total biomass from a free-air CO_2 enrichment (Figure 8). The results indicated that for the control (350 ppm) and high CO_2 (600 ppm), the simulations reproduced the difference in total biomass dynamics, and the 250-ppm enrichment of CO_2 concentration increased the simulated final biomass by 2% and 9% for the Summer–Autumn 2020 and the Spring–Winter 2021, respectively, which led to the yield increase.
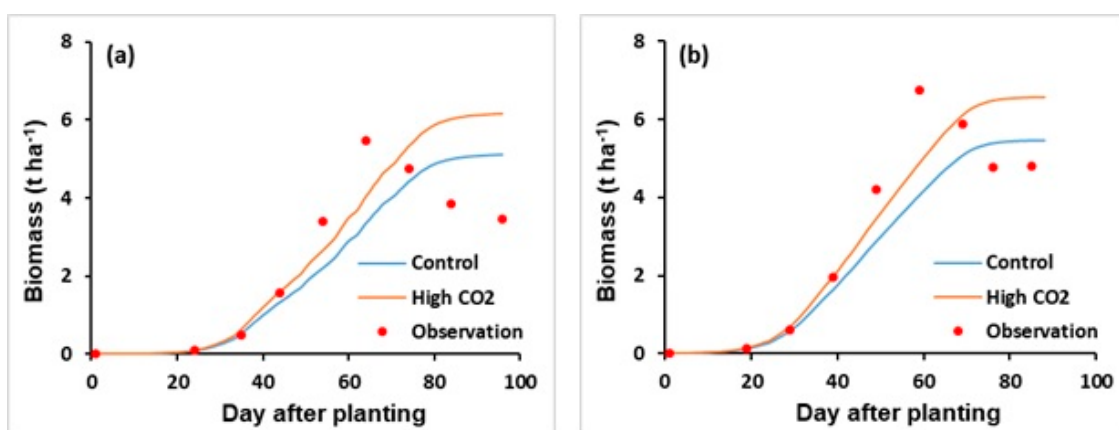

Figure 8. Total aboveground biomass under different atmospheric CO_2 concentrations for the control (350 ppm) and high CO_2 (600 ppm), and observed total biomass from the experiment site. (**a**) Summer-Autumn 2020; (**b**) Spring-Winter 2021.

Relative yield changes were simulated with increasing temperatures and CO_2 concentrations, as shown in Figure 9. The soybean yield rapidly decreased in the Summer–Autumn of 2020 with about a 7% reduction per °C increase, while in the Spring–Winter of 2021, this reduction was about 2.3% (Figure 9a). With an increase in the CO_2 concentration, the

yield increased by about 14% and 16% per 100 ppm for the Summer–Autumn 2020 and the Spring–Winter 2021, respectively (Figure 9b).
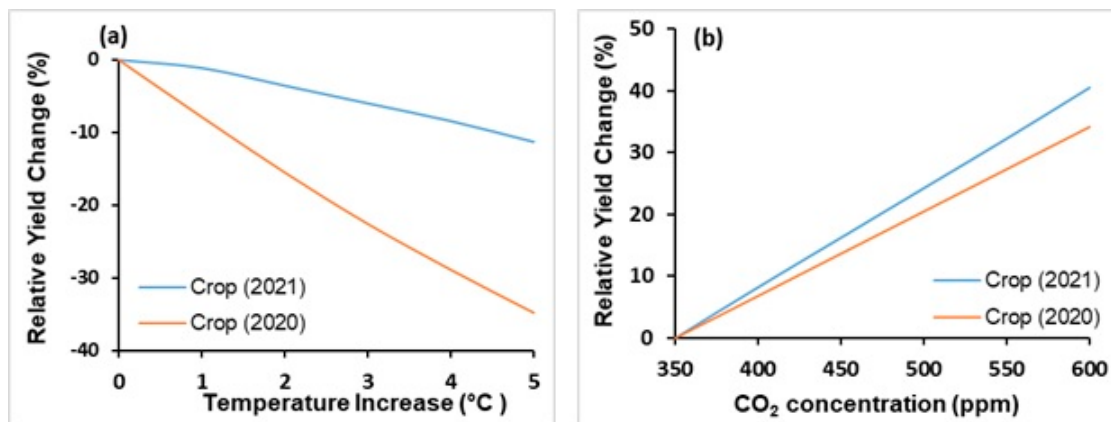

Figure 9. Simulated yields for soybean with (**a**) increasing temperature and (**b**) elevated atmospheric CO_2 concentration.

Besides temperature, CO_2 is an influencing factor on the yield. This study reported the yield enhancement by the CO_2 increase, which agreed with the report from historical analysis of the effects of CO_2 on the yield [53]. Zhao et al. [7] found a yield increase of 7% per 100 ppm CO_2 in the USA, which is lower than the case in our study. The yield can increase by up to 26–31% as the free-air CO_2 is enriched [54]. The phenomenon of the increase was also recorded in Pradesh, India [55], and Iowa, USA [56], particularly in major soybean production countries such as the USA, Brazil, and China [53].

The effects of elevated CO_2 on yield are fundamental to the fertilization effect [53]. Historical data analyses showed that the average yields for the USA, Brazil, and China in 2002–2006 (377 ppm CO_2 in 2006) were 4.34%, 7.57%, and 5.10% higher, respectively, than that in 1980 (338 ppm CO_2) [53]. In other words, fertilization can increase the yield, i.e., the level of 370 ppm CO_2 triggered the yield increase for Iowa, USA [57], and the soybean productivity enhancement [58]. The mechanism of this effect is that rising CO_2 levels can affect the photosynthesis capacity, photosynthetic pigment, and antioxidant levels at flowering stages, particularly at 400 ppm and 600 ppm levels of CO_2 [59]. In addition, the rising levels of CO_2 from 400 to 600 ppm can reduce Fe (negative correlation with the yield) in soybean seeds, which is the opposite to the elevated temperature [60]. In co-effects, the increase of 2.1 °C together with CO_2 of 700 ppm can increase the yield by 31% [61]. Such evidence showed that elevated CO_2 levels may boost the yield increase, which could be a potential benefit for future climates with high CO_2 concentrations in terms of soybean production. However, soybeans may be co-affected by temperature and CO_2, which further studies should consider.

4. Conclusions

The SIMPLE model performed well in assessing the soybean biomass and yield in this case study. It is a generic and simple dynamic model based on the known principles of crop physiology with a few equations and parameters. This model was competent for estimating the soybean yield under different weather conditions. This study found that drought stress inhibited the soybean growth, and although drought stress due to less rainfall seemed to be more serious in Spring–Winter 2021 than in Summer–Autumn 2020, the soybeans grown in rainy months have a longer growing period and lower yield than those planted in less rainy months under the same environmental conditions. An increase in temperature can lead to a yield reduction, while an increase in CO_2 can be followed by a yield increase. Modeling using the SIMPLE model is useful for assessing the responses of soybeans to

climate impacts, which can be applicable to other studies, particularly in tropical areas with similar climates.

References

1. El Bassam, N. *Handbook of Bioenergy Crops: A Complete Reference to Species, Development and Applications*; Routledge: Abingdon-on-Thames, UK, 2010.
2. Saryoko, A.; Homma, K.; Lubis, I.; Shiraiwa, T. Plant development and yield components under a tropical environment in soybean cultivars with temperate and tropical origins. *Plant Prod. Sci.* **2017**, *20*, 375–383. [CrossRef]
3. Kucharik, C.J.; Serbin, S.P. Impacts of recent climate change on Wisconsin corn and soybean yield trends. *Environ. Res. Lett.* **2008**, *3*, 034003. [CrossRef]
4. Zanon, A.J.; Streck, N.A.; Grassini, P. Climate and Management Factors Influence Soybean Yield Potential in a Subtropical Environment. *Agron. J.* **2016**, *108*, 1447–1454. [CrossRef]
5. Reis, L.; Santos e Silva, C.M.; Bezerra, B.; Mutti, P.; Spyrides, M.H.; Silva, P.; Magalhães, T.; Ferreira, R.; Rodrigues, D.; Andrade, L. Influence of climate variability on soybean yield in MATOPIBA, Brazil. *Atmosphere* **2020**, *11*, 1130. [CrossRef]
6. Khojely, D.M.; Ibrahim, S.E.; Sapey, E.; Han, T. History, current status, and prospects of soybean production and research in sub-Saharan Africa. *Crop J.* **2018**, *6*, 226–235. [CrossRef]
7. Zhao, C.; Liu, B.; Xiao, L.; Hoogenboom, G.; Boote, K.J.; Kassie, B.T.; Pavan, W.; Shelia, V.; Kim, K.S.; Hernandez-Ochoa, I.M.; et al. A SIMPLE crop model. *Eur. J. Agron.* **2019**, *104*, 97–106. [CrossRef]
8. Banterng, P.; Hoogenboom, G.; Patanothai, A.; Singh, P.; Wani, S.; Pathak, P.; Tongpoonpol, S.; Atichart, S.; Srihaban, P.; Buranaviriyakul, S. Application of the Cropping System Model (CSM)-CROPGRO-Soybean for Determining Optimum Management Strategies for Soybean in Tropical Environments. *J. Agron. Crop Sci.* **2010**, *196*, 231–242. [CrossRef]
9. Wu, X.; Vuichard, N.; Ciais, P.; Viovy, N.; de Noblet-Ducoudré, N.; Wang, X.; Magliulo, V.; Wattenbach, M.; Vitale, L.; Di Tommasi, P. ORCHIDEE-CROP (v0), a new process-based agro-land surface model: Model description and evaluation over Europe. *Geosci. Model Dev.* **2016**, *9*, 857–873. [CrossRef]
10. Li, Z.; Zhan, C.; Hu, S.; Ning, L.; Wu, L.; Guo, H. Evaluation of global gridded crop models (GGCMs) for the simulation of major grain crop yields in China. *Hydrol. Res.* **2022**, *53*, 353–369. [CrossRef]
11. Schauberger, B.; Archontoulis, S.; Arneth, A.; Balkovic, J.; Ciais, P.; Deryng, D.; Elliott, J.; Folberth, C.; Khabarov, N.; Müller, C.; et al. Consistent negative response of US crops to high temperatures in observations and crop models. *Nat. Commun.* **2017**, *8*, 13931. [CrossRef]
12. Goulart, H.M.; van der Wiel, K.; Folberth, C.; Boere, E.; van den Hurk, B. Increase of simultaneous soybean failures due to climate change. *Earth's Future* **2023**, *11*, e2022EF003106. [CrossRef]
13. Sun, Q.; Zhang, Y.; Che, X.; Chen, S.; Ying, Q.; Zheng, X.; Feng, A. Coupling Process-Based Crop Model and Extreme Climate Indicators with Machine Learning Can Improve the Predictions and Reduce Uncertainties of Global Soybean Yields. *Agriculture* **2022**, *12*, 1791. [CrossRef]
14. Kaul, M.; Hill, R.L.; Walthall, C. Artificial neural networks for corn and soybean yield prediction. *Agric. Syst.* **2005**, *85*, 1–18. [CrossRef]
15. Dasgupta, P. Chapter 5 Population, poverty, and the natural environment. In *Handbook of Environmental Economics*; Mäler, K.-G., Jeffrey, R.V., Eds.; Elsevier: Amsterdam, The Netherlands, 2003; Volume 1, pp. 191–247.
16. Phung, D.; Nguyen-Huy, T.; Tran, N.N.; Tran, D.N.; Nghiem, S.; Nguyen, N.H.; Nguyen, T.H.; Bennett, T. Hydropower dams, river drought and health effects: A detection and attribution study in the lower Mekong Delta Region. *Clim. Risk Manag.* **2021**, *32*, 100280. [CrossRef]
17. Monteith, J.L. Light Distribution and Photosynthesis in Field Crops. *Ann. Bot.* **1965**, *29*, 17–37. [CrossRef]
18. Ahmed, M.; Ahmad, S. *Systems Modeling*; Spinger: Singapore, 2020; pp. 1–44.
19. Ross, J. *The Radiation Regime and Architecture of Plant Stands*; Springer Science & Business Media: Berlin, Germany, 1981.
20. Asseng, S.; Foster, I.A.N.; Turner, N.C. The impact of temperature variability on wheat yields. *Glob. Chang. Biol.* **2011**, *17*, 997–1012. [CrossRef]

21. Bindi, M.; Fibbi, L.; Gozzini, B.; Orlandini, S.; Miglietta, F. Modelling the impact of future climate scenarios on yield and yield variability of grapevine. *Clim. Res.* **1996**, *7*, 213–224. [CrossRef]

22. Ewert, F.; Rodriguez, D.; Jamieson, P.; Semenov, M.A.; Mitchell, R.A.C.; Goudriaan, J.; Porter, J.R.; Kimball, B.A.; Pinter, P.J.; Manderscheid, R.; et al. Effects of elevated CO_2 and drought on wheat: Testing crop simulation models for different experimental and climatic conditions. *Agric. Ecosyst. Environ.* **2002**, *93*, 249–266. [CrossRef]

23. Priestley, C.H.B.; Taylor, R.J.F. On the Assessment of Surface Heat Flux and Evaporation Using Large-Scale Parameters. *Mon. Weather. Rev.* **1972**, *100*, 81–92. [CrossRef]

24. Ritchie, J.; Godwin, D.; Otter-Nacke, S. *CERES-Wheat: A User-Oriented Wheat Yield Model. Preliminary Documentation. AGRISTARS Publication No.: YM-U3-04442-JSC-18892*; Michigan State University: East Lansing, MI, USA, 1985.

25. van Ittersum, M.K.; Howden, S.M.; Asseng, S. Sensitivity of productivity and deep drainage of wheat cropping systems in a Mediterranean environment to changes in CO_2, temperature and precipitation. *Agric. Ecosyst. Environ.* **2003**, *97*, 255–273. [CrossRef]

26. Woli, P.; Jones, J.W.; Ingram, K.T.; Fraisse, C.W. Agricultural Reference Index for Drought (ARID). *Agron. J.* **2012**, *104*, 287–300. [CrossRef]

27. Sinclair, T.R.; Tanner, C.B.; Bennett, J.M. Water-Use Efficiency in Crop Production. *BioScience* **1984**, *34*, 36–40. [CrossRef]

28. Steduto, P.; Hsiao, T.C.; Raes, D.; Fereres, E. AquaCrop—The FAO Crop Model to Simulate Yield Response to Water: I. Concepts and Underlying Principles. *Agron. J.* **2009**, *101*, 426–437. [CrossRef]

29. Wnuk, A.; Górny, A.; Bocianowski, J.; Kozak, M. Visualizing harvest index in crops. *Commun. Biometry Crop Sci.* **2013**, *8*, 48–59.

30. Milton, E.P.-F.; Flávio, B.J. Yield Components and Biomass Partition in Soybean: Climate Change Vision. In *Soybean-Biomass, Yield and Productivity*; Intechopen: London, UK, 2019.

31. Whigham, D.K.; Minor, H.C. 4-Agronomic Characteristics and Environmental Stress. In *Soybean Physiology, Agronomy, and Utilization*; Norman, A.G., Ed.; Academic Press: Cambridge, MA, USA, 1978; pp. 77–118.

32. Ries, L.L.; Purcell, L.C.; Carter, T.E., Jr.; Edwards, J.T.; King, C.A. Physiological Traits Contributing to Differential Canopy Wilting in Soybean under Drought. *Crop Sci.* **2012**, *52*, 272–281. [CrossRef]

33. Munoz, G.; Maraux, F.; Wahaj, R. *Actual Crop Water Use in Project Countries a Synthesis at the Regional Level*; The World Bank: Washington, DC, USA, 2007.

34. Jamieson, P.D.; Porter, J.R.; Wilson, D.R. A test of the computer simulation model ARCWHEAT1 on wheat crops grown in New Zealand. *Field Crops Res.* **1991**, *27*, 337–350. [CrossRef]

35. Adeboye, O.B.; Schultz, B.; Adekalu, K.O.; Prasad, K.C. Performance evaluation of AquaCrop in simulating soil water storage, yield, and water productivity of rainfed soybeans (*Glycine max* L. merr) in Ile-Ife, Nigeria. *Agric. Water Manag.* **2019**, *213*, 1130–1146. [CrossRef]

36. Liu, S.; Yang, J.Y.; Zhang, X.Y.; Drury, C.F.; Reynolds, W.D.; Hoogenboom, G. Modelling crop yield, soil water content and soil temperature for a soybean–maize rotation under conventional and conservation tillage systems in Northeast China. *Agric. Water Manag.* **2013**, *123*, 32–44. [CrossRef]

37. Gaso, D.V.; de Wit, A.; Berger, A.G.; Kooistra, L. Predicting within-field soybean yield variability by coupling Sentinel-2 leaf area index with a crop growth model. *Agric. For. Meteorol.* **2021**, *308–309*, 108553. [CrossRef]

38. Yang, Q.; Wang, K.; Kang, J.; Liang, F. Effects of rainfall, temperature and illumination on outcrossing rate of male sterile line in soybean. *Oil Crop Sci.* **2020**, *5*, 17–21. [CrossRef]

39. Matthews, E.R.; Mazer, S.J. Historical changes in flowering phenology are governed by temperature $\times$ precipitation interactions in a widespread perennial herb in western North America. *New Phytol.* **2016**, *210*, 157–167. [CrossRef]

40. Smith, J. *Crop, Pasture and Timber Yield Index. Cedara Report N/A/94/4*; Natal Agricultural Research Institute: Cedara, South Africa, 1994.

41. Schlenker, W.; Roberts, M.J. Nonlinear temperature effects indicate severe damages to US crop yields under climate change. *Proc. Natl. Acad. Sci. USA* **2009**, *106*, 15594–15598. [CrossRef]

42. Wiebbecke, C.E.; Graham, M.A.; Cianzio, S.R.; Palmer, R.G. Day temperature influences the male-sterile locus ms9 in soybean. *Crop Sci.* **2012**, *52*, 1503–1510. [CrossRef]

43. Caviness, C.; Fagala, B. Influence of Temperature on a Partially Male-Sterile Soybean Strain 1. *Crop Sci.* **1973**, *13*, 503–504. [CrossRef]

44. Allen, L.H.; Zhang, L.; Boote, K.J.; Hauser, B.A. Elevated temperature intensity, timing, and duration of exposure affect soybean internode elongation, mainstem node number, and pod number per plant. *Crop J.* **2018**, *6*, 148–161. [CrossRef]

45. Liu, Y.; Dai, L. Modelling the impacts of climate change and crop management measures on soybean phenology in China. *J. Clean. Prod.* **2020**, *262*, 121271. [CrossRef]

46. Wang, X.; Zhao, C.; Müller, C.; Wang, C.; Ciais, P.; Janssens, I.; Peñuelas, J.; Asseng, S.; Li, T.; Elliott, J. Emergent constraint on crop yield response to warmer temperature from field experiments. *Nat. Sustain.* **2020**, *3*, 908–916. [CrossRef]

47. Burroughs, C.H.; Montes, C.M.; Moller, C.A.; Mitchell, N.G.; Michael, A.M.; Peng, B.; Kimm, H.; Pederson, T.L.; Lipka, A.E.; Bernacchi, C.J.; et al. Reductions in leaf area index, pod production, seed size, and harvest index drive yield loss to high temperatures in soybean. *J. Exp. Bot.* **2022**, *74*, 1629–1641. [CrossRef] [PubMed]

48. Leng, G.; Hall, J. Crop yield sensitivity of global major agricultural countries to droughts and the projected changes in the future. *Sci. Total Environ.* **2019**, *654*, 811–821. [CrossRef]

49. Fernandes, R.D.M.; de Melo, D.M.; Elli, E.F.; Battisti, R. Climate change impacts on rainfed and irrigated soybean yield in Brazil's new agricultural frontier. *Theor. Appl. Climatol.* **2022**, *147*, 803–816. [CrossRef]

50. Alsajri, F.A.; Wijewardana, C.; Bheemanahalli, R.; Irby, J.T.; Krutz, J.; Golden, B.; Reddy, V.R.; Reddy, K.R. Morpho-physiological, yield, and transgenerational seed germination responses of soybean to temperature. *Front. Plant Sci.* **2022**, *13*, 839270. [CrossRef]

51. Jumrani, K.; Bhatia, V.S. Interactive effect of temperature and water stress on physiological and biochemical processes in soybean. *Physiol. Mol. Biol. Plants* **2019**, *25*, 667–681. [CrossRef] [PubMed]

52. Casali, L.; Herrera, J.M.; Rubio, G. Resilient soybean and maize production under a varying climate in the semi-arid and sub-humid Chaco. *Eur. J. Agron.* **2022**, *135*, 126463. [CrossRef]

53. Sakurai, G.; Iizumi, T.; Nishimori, M.; Yokozawa, M. How much has the increase in atmospheric CO_2 directly affected past soybean production? *Sci. Rep.* **2014**, *4*, 4978. [CrossRef]

54. Hao, X.; Gao, J.; Han, X.; Ma, Z.; Merchant, A.; Ju, H.; Li, P.; Yang, W.; Gao, Z.; Lin, E. Effects of open-air elevated atmospheric CO_2 concentration on yield quality of soybean (*Glycine max* (L.) Merr). *Agric. Ecosyst. Environ.* **2014**, *192*, 80–84. [CrossRef]

55. Lal, M.; Singh, K.K.; Srinivasan, G.; Rathore, L.S.; Naidu, D.; Tripathi, C.N. Growth and yield responses of soybean in Madhya Pradesh, India to climate variability and change. *Agric. For. Meteorol.* **1999**, *93*, 53–70. [CrossRef]

56. Haskett, J.D.; Pachepsky, Y.A.; Acock, B. Increase of CO_2 and Climate Change Effects on Iowa Soybean Yield, Simulated Using GLYCIM. *Agron. J.* **1997**, *89*, 167–176. [CrossRef]

57. Srivastava, A.; McGhee, R.P.; Flanagan, D.C.; Frankenberger, J.R.; Engel, B.A. Modeling the Impacts of Climate change on Crop Yield, Runoff, and Soil Loss Using the Water Erosion Prediction Project (WEPP) Model. In *Soil Erosion Research Under a Changing Climate, January 8–13, 2023, Aguadilla, Puerto Rico*; ASABE: St. Joseph, MI, USA, 2023.

58. Thomey, M.L.; Slattery, R.A.; Köhler, I.H.; Bernacchi, C.J.; Ort, D.R. Yield response of field-grown soybean exposed to heat waves under current and elevated [CO_2]. *Glob. Chang. Biol.* **2019**, *25*, 4352–4368. [CrossRef]

59. Li, B.; Feng, Y.; Zong, Y.; Zhang, D.; Hao, X.; Li, P. Elevated CO_2-induced changes in photosynthesis, antioxidant enzymes and signal transduction enzyme of soybean under drought stress. *Plant Physiol. Biochem.* **2020**, *154*, 105–114. [CrossRef]

60. Köhler, I.H.; Huber, S.C.; Bernacchi, C.J.; Baxter, I.R. Increased temperatures may safeguard the nutritional quality of crops under future elevated CO_2 concentrations. *Plant J.* **2019**, *97*, 872–886. [CrossRef]

61. Qiao, Y.; Miao, S.; Li, Q.; Jin, J.; Luo, X.; Tang, C. Elevated CO_2 and temperature increase grain oil concentration but their impacts on grain yield differ between soybean and maize grown in a temperate region. *Sci. Total Environ.* **2019**, *666*, 405–413. [CrossRef] [PubMed]